

Electromagnetic Optimization of 3-D Structures

John W. Bandler, *Fellow, IEEE*, Radoslaw M. Biernacki, *Fellow, IEEE*, Shao Hua Chen, *Senior Member, IEEE*, Louis W. Hendrick, and Dževat Omeragić, *Member, IEEE*

Abstract—This paper discusses novel techniques and methodologies suitable for automated electromagnetic (EM) design of arbitrary three-dimensional (3-D) structures. In the context of parameterization of arbitrary 3-D structures, the authors outline the concept of the geometry capture technique. The authors present efficient response interpolation with respect to optimizable parameters—the key to effective automation. The authors' formulation is based on the maximally flat quadratic interpolation (MFQI) technique and provides gradient estimation essential to efficient optimization. The authors address the issue of storing the results of expensive EM simulations in a dynamically updated database, integrated with the interpolation technique. The automated EM optimization process is illustrated by the design of waveguide mitered bends. The authors also apply the aggressive space mapping (SM) technique to the optimization of multistep waveguide transformers.

Index Terms— Design automation, electromagnetic analysis, finite-element methods, optimization methods, waveguide bends.

I. INTRODUCTION

TECHNOLOGICAL revolutions in the field of microwave and communication systems are pushing requirements for further circuit compaction and the exploitation of electromagnetics-based computer-aided design (CAD). Further innovative designs may be achieved using powerful three-dimensional (3-D) full-wave electromagnetic (EM) simulators in conjunction with sophisticated optimization algorithms [1]. EM simulators, whether stand-alone or incorporated into software frameworks, will not realize their full potential to the designer unless they are optimizer-driven to automatically adjust designable parameters. The advancement of computer technology and development of appropriate algorithms and techniques make possible the use of fully 3-D simulators first in validation and then in the optimization process [2]. The use of the field-theoretic approach in design strongly complements conventional CAD using circuit simulators. Combined use of both is rapidly becoming common practice for first-pass success design.

Manuscript received January 23, 1997; revised January 28, 1997. This work was supported in part by Optimization Systems Associates, Inc. and in part by the Natural Sciences and Engineering Research Council of Canada under Grant OGP007239, Grant OGP0042444, and Grant STR0167080, and through the Micronet Network of Centres of Excellence.

J. W. Bandler, R. M. Biernacki, S. H. Chen, and D. Omeragić are with the Simulation Optimization Systems Research Laboratory and the Department of Electrical and Computer Engineering, McMaster University, Hamilton, Ont., Canada L8S 4L7, and also with Optimization Systems Associates, Inc., Dundas, Ont., Canada L9H 5E7.

L. W. Hendrick is with the Antenna/Microwave Business Unit, Hughes Space and Communications Company, Los Angeles, CA 90009 USA.

Publisher Item Identifier S 0018-9480(97)03107-4.

For practical EM optimization, several key factors in the development of efficient CAD software have been identified [3], [4]. Besides what are considered common CAD software necessities, such as user-friendly interfaces, efficient numerical algorithms, and open architecture, the software designer and the advanced user of optimization software must have efficient tools for interprocess communication, methodologies for design parameterization, geometrical interpolation and modeling techniques, and efficient database organization and handling.

New techniques, such as geometry capture [5] and space mapping (SM) [2], [6], [7], in conjunction with efficient interpolation, intelligent database, and Datapipe architecture establish a solid foundation for efficient optimization of 3-D structures. SM has to be "aggressive," since computational costs are extremely high, while geometry capture has to be fully implemented in 3-D. Recent advances in these two techniques are discussed elsewhere in more detail [8], [5].

This paper is devoted to optimization concepts and algorithms suitable for automated EM optimization of 3-D structures. Section II provides the background relevant to the implementation of various optimization concepts to 3-D design. It is followed in Section III by an outline of the authors' approach addressing the critical issue [9] of parameterization of geometrical structures in automated EM optimization. Section IV describes the interpolation technique which is a key to effective automation and efficient optimization. Called maximally flat quadratic interpolation (MFQI), it is applied here to the creation of interpolation models of EM responses of 3-D structures. Complete formulas for the linear and quadratic case are presented. In Section V, the authors give details of the gradient estimation process, based on their interpolation method. The database organization and implementation is discussed in Section VI.

Following the theoretical concepts, Sections VII and VIII offer EM design optimization of waveguiding structures to illustrate the methodologies. As an illustration of practical 3-D design including geometry capture, the authors present results of successful optimization of WR-75 mitered bends. Waveguide transformers are optimized using the automated aggressive SM. The results presented in this paper have been obtained using Empipe3D [10], which uses the optimization engine of OSA90/hope [10] to drive the commercial high-frequency structure simulators (HFSS) [11] and Ansoft's Maxwell Eminence [12]. The paper concludes with suggestions for further development.

II. BACKGROUND ON EM OPTIMIZATION OF 3-D STRUCTURES

The implementation of optimization-related algorithms is dependent on the particular EM field solver used. Import-

tant techniques for solving 3-D EM fields are based on: the finite-element method (FEM)—commercial simulators include HFSS [11], Maxwell Eminence [12], MagNet [13], MicroWave Lab [14]; the integral equation (boundary-element) method (IE/BEM) [15], [16]; the transmission-line method (TLM) [17]; the finite-difference time-domain method (FDTD) [18], [19]; the mode-matching (MM) method [20], [21]; and the method of moments (MoM) [22], [23]. Each of these methods has its own advantages and disadvantages and is suitable for a specific class of problems [24].

Two approaches are available to implement optimization using full-wave 3-D EM simulators [25]. The first is the exploitation of commercial EM software packages such as HFSS or Maxwell Eminence inside the optimization loop of a general purpose optimization program. In microwave monolithic integrated circuit (MMIC) design, circuit optimization packages such as HP-EEsof's Touchstone [26] and OSA90/hope are routinely used. OSA90/hope provides users the opportunity of interfacing external simulators using UNIX-based Datapipe technology. Through the Empipe software [10] OSA90/hope is interfaced to Sonnet Software's *em* [27], a widely used full-wave EM simulator based on the MoM, created for the design of predominantly planar structures. The interfacing to truly 3-D simulators based on FEM, TLM, and MM has been recently reported [1], [2]. This represents a major advance in CAD.

The second approach is based on formulating optimization at a lower level, i.e., using properties of a numerical approximation method in order to derive corresponding sensitivity matrices to be used in the optimization process. Sensitivity of the design could be based on differentiation of base equations obtained after discretization of differential or integral operators using the FEM [28], [29] or the MoM [30], [31]. Another possibility is the adjoint network concept [32]–[34]. It provides an elegant approach to computing derivatives of objective functions, requiring only one full simulation to evaluate gradients for reciprocal structures. Its efficiency increases with the number of optimization variables; it, therefore, has the potential of reducing the central processing unit (CPU) time significantly.

Both variants of the adjoint approach are still under development and a subject of research. Ideas are already implemented in two-dimensional (2-D) low-frequency magnetics [35]–[38] and to optimize the design of certain waveguiding structures [25], [29], [39], [40]. In the microwave area, Sorrentino and his collaborators integrated the adjoint network technique with the MM [32], [33]. They basically applied the circuit theory concept directly to the MM formulation based on a generalized admittance matrix formulation [33]. Dyck, Lowther, and Freeman derived a Tellegen's theorem for field equations [34], and applied the adjoint variable concept to the 2-D low-frequency inverse problem. All referenced work [25], [28]–[40] is mostly academic. There does not appear to be a general purpose commercial software package based on the adjoint network method.

In the optimization process of low-frequency magnetic devices, the problem of finding a global minimum is being addressed. Global optimization techniques such as simulated

annealing, genetic algorithms, fuzzy systems, and an artificial intelligence approach have been attempted. The ease of implementation makes them attractive, but their efficiency is questionable. Extremely high computational costs have to be justified even for 2-D potential problems, since the number of simulations is of the order of 10^2 – 10^3 . These methods could be used to localize the global minimum, and then efficient gradient-based methods should be used. The choice of the starting point for optimization is another important aspect of CAD, with the possibility of the application of knowledge-based methods and neural networks [41].

When FEM-based simulators are used, the geometry of the structure being adjusted is discretized using automatic mesh generators, independently in each step. As a consequence, estimated gradients of response functions may appear to be discontinuous. In order to achieve smooth gradients, parameterization could be integrated with the mesh generation stage. An efficient technique has been implemented for 2-D geometries [25].

III. PARAMETERIZATION OF 3-D STRUCTURES

As the optimization process proceeds, revised structures must be automatically generated. Moreover, each such structure must be physically meaningful and should follow the designer's intention with respect to allowable modifications and possible limits. EM simulators deal directly with the layout representation of circuits in terms of absolute coordinates which are not directly designable parameters. Therefore, one must be able to relate geometrical coordinates of the layout to the numerical parameters for optimization.

In order to take full advantage of superior accuracy of EM simulators and their ability to solve arbitrary geometries, the microwave designer expects to be able to optimize increasingly more complex structures. Geometrical parameterization is thus needed for every new structure and it is of utmost importance to leave this process to the user. Naturally, EM simulator users wish to be able to designate optimizable parameters directly within the graphical layout representation. To provide a tool addressing such structure parameterization the authors have developed the geometry capture technique, described in detail elsewhere [5].

Using geometry capture, optimizable parameters of an arbitrary EM structure are captured from a set of EM simulator's project (geometry and material description) files created by the user. These projects include a nominal project and number of perturbed projects, representing incremental changes for each optimization variable. The geometry capture technique facilitates automatic translation of the values of user-defined designable parameters to the layout description in terms of absolute coordinates. During optimization, this translation is automatically performed for each new set of parameter values before the EM simulator is invoked.

IV. RESPONSE INTERPOLATION

The 3-D structure parameters are discretized in order to improve the efficiency of the design optimization process. The responses obtained at discrete values of parameters are

interpolated. The benefits of this approach include efficient gradient evaluation, handling of tolerances, efficient model evaluation in Monte Carlo analysis, and yield-driven design [42].

The vector ϕ of structure parameters (all designable, or optimization, variables) can be written as

$$\phi = [\phi_1 \ \phi_2 \ \cdots \ \phi_n]^T \quad (1)$$

which may also include material parameters in addition to geometrical parameters.

Numerical EM simulation is performed at discrete values of structure parameters

$$\phi_i = k_i d_i, \quad i = 1, 2, \dots, n \quad (2)$$

where d_i is a discretization step, and k_i is an integer, typically positive. Equation (2), for all values of k_i , defines the discretization grid in the space of structure parameters. It should not be confused with the meshing scheme for FEM, FDTD, MoM, etc., and is independent of that scheme unless a fixed mesh is imposed on the physical structure.

The discretization matrix is defined as

$$D = \text{diag}\{d_i\}. \quad (3)$$

For off-grid structure parameter values interpolation of circuit responses is performed. Let one of the responses of interest be denoted by $R(\phi)$. It is assumed that $R(\phi)$ is real, e.g., magnitude of scattering parameter S_{11} . To interpolate the response the structure needs to be simulated at $K + 1$ base points defined by the *interpolation base matrix* B

$$B = [\phi^c \ \phi^1 \ \phi^2 \ \cdots \ \phi^K] \quad (4)$$

where ϕ^i represents a given point (vector) of designable (optimization) variables, with components given by (1). To emphasize the fact that the simulation results at the base points are obtained from an EM solver the responses will be denoted by R_{EM} , e.g., $R_{\text{EM}}(\phi^c)$. As in [3], ϕ^c is called the *center base point*, which is the grid point nearest to the current point ϕ as determined by

$$\phi = \phi^c + D\Theta\mathbf{u} \quad (5)$$

where the *relative deviation matrix* Θ is defined as

$$\Theta = \text{diag}\{\theta_i\} \quad (6)$$

with its entries constrained by the inequalities

$$-0.5 \leq \theta_i < 0.5, \quad i = 1, 2, \dots, n \quad (7)$$

and $\mathbf{u} = [1 \ 1 \ \cdots \ 1]^T$. ϕ^c and Θ can be easily determined using the “floor” function as

$$\phi_i^c = \left\lfloor \frac{\phi_i}{d_i} + 0.5 \right\rfloor d_i \quad (8)$$

and, then

$$\theta_i = \frac{\phi_i - \phi_i^c}{d_i}. \quad (9)$$

For convenience, the *relative deviation vector* θ is defined as

$$\theta = \Theta\mathbf{u}. \quad (10)$$

The remaining points in the interpolation base (column vectors in B) are defined by means of the *relative interpolation base matrix* B^n

$$B^n = [\eta^1 \ \eta^2 \ \cdots \ \eta^K] \quad (11)$$

where the vectors η^i are all different from $\mathbf{0}$, different from each other, and composed of $+1$, -1 , or 0 entries. The base points in B , by definition, are related to the center base point and the vectors η^i through the expressions

$$\phi^i = \phi^c + D\eta^i, \quad i = 1, 2, \dots, K. \quad (12)$$

The selection of B^n and of the number of additional base points K depends on the interpolation scheme to be considered.

A *validity region* V for the current interpolation base (4) shall be defined. If the point ϕ moves outside the current validity region a new interpolation base (possibly overlapping with the current one) needs to be selected.

Following [3], one considers the class of interpolation problems where the interpolating function can be expressed as a linear combination of some *fundamental interpolating functions* in terms of deviations with respect to the center base point, so that

$$R(\phi) = R_{\text{EM}}(\phi^c) + \mathbf{f}^T(D\theta)\mathbf{a} \quad (13)$$

where \mathbf{a} contains the interpolation coefficients and \mathbf{f} is the vector of the fundamental interpolating functions. In the current implementation are considered two interpolation schemes: 1) linear and 2) MFQI [43], [44].

For the linear interpolation one may define the fundamental interpolating functions as

$$\mathbf{f}(\mathbf{x}) = \mathbf{x} \quad (14)$$

and, given ϕ (and correspondingly Θ), the relative interpolation base is selected as

$$B^n = \text{sign} \ \Theta. \quad (15)$$

Here $K = n$. The validity region V , in this case, is the corresponding multidimensional quadrant of the region defined by the inequalities (7), i.e.,

$$-1 + \text{sign}(\theta_i) \leq 4\theta_i < 1 + \text{sign}(\theta_i), \quad i = 1, 2, \dots, n. \quad (16)$$

Fig. 1(a) illustrates in two dimensions the selection of the base points according to (15), as well as the corresponding validity region. For (13) to hold exactly at all the base points (15), i.e., $R(\phi^i) = R_{\text{EM}}(\phi^i)$, one has the equations

$$\eta^{iT} D\mathbf{a} = R_{\text{EM}}(\phi^i) - R_{\text{EM}}(\phi^c), \quad i = 1, 2, \dots, n \quad (17)$$

or, in the matrix form $B^n D\mathbf{a} = \Delta R_{\text{EM}}(B)$, where $\Delta R_{\text{EM}}(B)$ is defined by (18) at the bottom of the next page. After solving (17) for \mathbf{a} and substituting into (13) one has

$$R(\phi) = R_{\text{EM}}(\phi^c) + \theta^T \text{sign} \ \Theta \Delta R_{\text{EM}}(B) \quad (19)$$

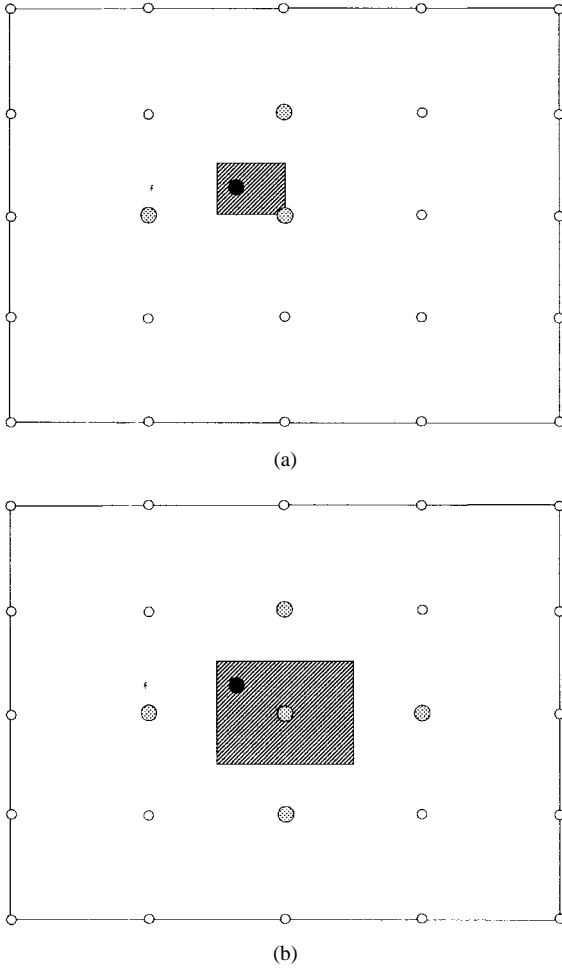


Fig. 1. The interpolation base points (shaded) needed for interpolation of an off-grid point (solid). Shaded rectangles are the corresponding validity regions. (a) Linear interpolation. (b) MFQI.

where one takes advantage of $\mathbf{B}^{\eta T} = (\mathbf{B}\eta)^{-1} = \mathbf{B}^{\eta}$ since \mathbf{B}^{η} is a diagonal matrix with $+1$ and -1 entries.

For the MFQI scheme, one may select the relative interpolation base by setting

$$\mathbf{B}^{\eta} = [\mathbf{1} \quad -\mathbf{1}] \quad (20)$$

where $\mathbf{1}$ is the $n \times n$ identity matrix. Here $K = 2n$. In this case, the validity region is established by the inequalities (7). Fig. 1(b) illustrates in two dimensions the selection of the base points according to (20), as well as the corresponding validity region. From earlier developments on MFQI [44] it is known that by this selection the mixed second-order terms will be conveniently set to zero in this type of interpolation. Therefore, the fundamental interpolating functions can be defined as

$$\mathbf{f}^T(\mathbf{x}) = [\mathbf{x}^T \quad \mathbf{x}^T \mathbf{X}] \quad (21)$$

where $\mathbf{X} = \text{diag} \{x_i\}$, or, in the form applicable to (13), as

$$\mathbf{f}^T(\mathbf{D}\boldsymbol{\theta}) = [\boldsymbol{\theta}^T \mathbf{D} \quad \mathbf{u}^T \boldsymbol{\theta}^2 \mathbf{D}^2]. \quad (22)$$

If the interpolation coefficient vector is partitioned as

$$\mathbf{a}^T = [\mathbf{a}_L^T \quad \mathbf{a}_Q^T] \quad (23)$$

where \mathbf{a}_L and \mathbf{a}_Q are the subvectors of \mathbf{a} corresponding to the linear and quadratic terms, respectively, then the system of equation at all the base points defined by (20) can be written as

$$\mathbf{D}\mathbf{a}_L + \mathbf{D}^2\mathbf{a}_Q = \Delta\mathbf{R}_{\text{EM}}^+ \quad (24a)$$

$$-\mathbf{D}\mathbf{a}_L + \mathbf{D}^2\mathbf{a}_Q = \Delta\mathbf{R}_{\text{EM}}^- \quad (24b)$$

where $\Delta\mathbf{R}_{\text{EM}}^+$ and $\Delta\mathbf{R}_{\text{EM}}^-$ are shown in (25) and (26), at the bottom of the next page. The solution of (24) is

$$\mathbf{a}_L = \frac{1}{2} \mathbf{D}^{-1} (\Delta\mathbf{R}_{\text{EM}}^+ - \Delta\mathbf{R}_{\text{EM}}^-) \quad (27a)$$

$$\mathbf{a}_Q = \frac{1}{2} \mathbf{D}^{-2} (\Delta\mathbf{R}_{\text{EM}}^+ + \Delta\mathbf{R}_{\text{EM}}^-) \quad (27b)$$

which, after substituting to (13), gives

$$\begin{aligned} R(\boldsymbol{\phi}) &= R_{\text{EM}}(\boldsymbol{\phi}^c) + \boldsymbol{\theta}^T \mathbf{D} \frac{1}{2} \mathbf{D}^{-1} (\Delta\mathbf{R}_{\text{EM}}^+ - \Delta\mathbf{R}_{\text{EM}}^-) \\ &\quad + \boldsymbol{\theta}^T \mathbf{D}^2 \boldsymbol{\theta} \frac{1}{2} \mathbf{D}^{-2} (\Delta\mathbf{R}_{\text{EM}}^+ + \Delta\mathbf{R}_{\text{EM}}^-) \end{aligned} \quad (28)$$

or

$$\begin{aligned} R(\boldsymbol{\phi}) &= R_{\text{EM}}(\boldsymbol{\phi}^c) + \frac{1}{2} \boldsymbol{\theta}^T (\Delta\mathbf{R}_{\text{EM}}^+ - \Delta\mathbf{R}_{\text{EM}}^-) \\ &\quad + \frac{1}{2} \boldsymbol{\theta}^T \boldsymbol{\theta} (\Delta\mathbf{R}_{\text{EM}}^+ + \Delta\mathbf{R}_{\text{EM}}^-). \end{aligned} \quad (29)$$

The interpolation schemes combining linear and MFQI interpolations and using the number of base points $n < K < 2n$ can also be derived using the similar approach.

V. GRADIENT ESTIMATION

To apply gradient-based optimizers, one needs to provide the gradients of the objective function. This involves evaluation of the gradients of $R(\boldsymbol{\phi})$. Since the fundamental interpolating functions are known, their gradients are available in analytical form. Therefore, from (5) and (13), one can calculate the gradient of $R(\boldsymbol{\phi})$ for the optimizer from the gradients of \mathbf{f} as

$$\frac{\partial R(\boldsymbol{\phi})}{\partial \boldsymbol{\phi}} = \mathbf{D}^{-1} \frac{\partial}{\partial \boldsymbol{\theta}} [\mathbf{f}^T(\mathbf{D}\boldsymbol{\theta})\mathbf{a}]. \quad (30)$$

For the linear interpolation case

$$\frac{\partial R(\boldsymbol{\phi})}{\partial \boldsymbol{\phi}} = \mathbf{D}^{-1} \text{sign } \boldsymbol{\theta} \Delta\mathbf{R}_{\text{EM}}(\mathbf{B}) \quad (31)$$

and

$$\begin{aligned} \frac{\partial R(\boldsymbol{\phi})}{\partial \boldsymbol{\phi}} &= \frac{1}{2} \mathbf{D}^{-1} (\Delta\mathbf{R}_{\text{EM}}^+ - \Delta\mathbf{R}_{\text{EM}}^-) \\ &\quad + \mathbf{D}^{-1} \boldsymbol{\theta} (\Delta\mathbf{R}_{\text{EM}}^+ + \Delta\mathbf{R}_{\text{EM}}^-) \end{aligned} \quad (32)$$

in the case of MFQI.

Some optimizers may request perturbed simulation in the vicinity of the nominal point $\boldsymbol{\phi}^0$, say at $\boldsymbol{\phi}^{\text{pert}}$, in order to estimate the gradient by perturbation, instead of using the gradient at $\boldsymbol{\phi}^0$ directly. For linear interpolation the perturbation technique will produce the same results as (30) as long as the interpolation base for the calculation of $\boldsymbol{\phi}^{\text{pert}}$ is kept the same as that of $\boldsymbol{\phi}^0$. This can be easily enforced even if $\boldsymbol{\phi}^{\text{pert}}$

$$\Delta\mathbf{R}_{\text{EM}}(\mathbf{B}) = [R_{\text{EM}}(\boldsymbol{\phi}^1) - R_{\text{EM}}(\boldsymbol{\phi}^c) \quad R_{\text{EM}}(\boldsymbol{\phi}^2) - R_{\text{EM}}(\boldsymbol{\phi}^c) \quad \cdots \quad R_{\text{EM}}(\boldsymbol{\phi}^K) - R_{\text{EM}}(\boldsymbol{\phi}^c)]^T \quad (18)$$

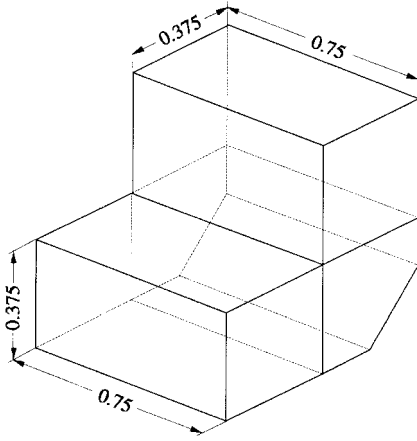
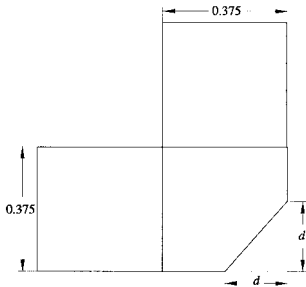


Fig. 2. Geometry of the optimized WR-75 mitered bend.

Fig. 3. Definition of the optimization variable d .

falls outside the validity region of ϕ^0 . In the case of quadratic interpolation, using (29) at ϕ^{pert} may provide a different result from (32). As the exact gradient (32) is available, a modified response at ϕ^{pert} can be easily evaluated from the linearized interpolating function at ϕ^0 as

$$\begin{aligned} R(\phi^{\text{pert}}) &= R_{\text{EM}}(\phi^c) + \frac{1}{2} \theta^{0T} (\Delta R_{\text{EM}}^+ - \Delta R_{\text{EM}}^-) \\ &+ \frac{1}{2} \theta^{0T} \theta^0 (\Delta R_{\text{EM}}^+ + \Delta R_{\text{EM}}^-) + (\phi^{\text{pert}} - \phi^0)^T \\ &\cdot \left\{ \frac{1}{2} D^{-1} (\Delta R_{\text{EM}}^+ - \Delta R_{\text{EM}}^-) + D^{-1} \theta^0 (\Delta R_{\text{EM}}^+ + \Delta R_{\text{EM}}^-) \right\} \end{aligned} \quad (33)$$

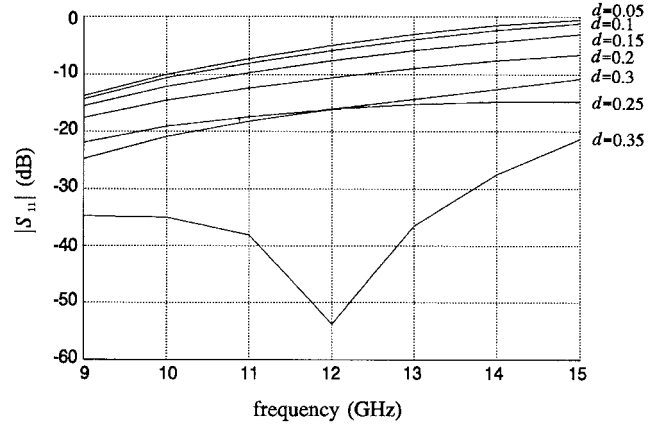
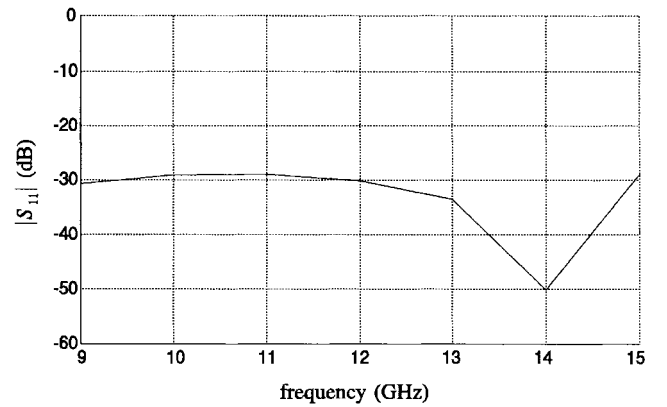
further simplifying to

$$\begin{aligned} R(\phi^{\text{pert}}) &= R_{\text{EM}}(\phi^c) + \frac{1}{2} \theta^{\text{pert}T} (\Delta R_{\text{EM}}^+ - \Delta R_{\text{EM}}^-) \\ &+ (\theta^{\text{pert}} - \frac{1}{2} \theta^0)^T \theta^0 (\Delta R_{\text{EM}}^+ + \Delta R_{\text{EM}}^-). \end{aligned} \quad (34)$$

This formula, when used in gradient estimation by perturbation, will produce the same result as (32).

VI. THE INTEGRATED DATABASE OF SIMULATION RESULTS

For an effective optimization process, it is necessary to efficiently utilize the results of EM simulations and to avoid repeated simulations. To achieve this, a database of already

Fig. 4. Brute-force approach: d varied from 0.05 to 0.35 in.Fig. 5. Response of the optimal bend with a single-section miter: $d_{\text{opt}} = 0.2897$ in.

simulated base points together with the corresponding responses is maintained.

Given an off-grid point, the validity region has to be determined by computing the center base point ϕ^c and the relative deviation vector θ using (8) and (9). The corresponding interpolation base (4) is generated using relative interpolation base matrices, defined by (15) or (20), depending on the interpolation technique. The interpolation base has to be checked against the stored database. Such EM simulation is invoked only for base points not present in the database. A simulation is followed by the update of the database. Results for base points already present in the database are simply retrieved and used for interpolation. After necessary responses are computed, response difference vectors ΔR_{EM} , defined by (18) for the linear case and (25) and (26) for the MFQI case, are generated. Then, interpolation of responses, based on (19) or (29), is performed, subsequently followed by computation of gradients using either (31) for the linear model or (32) for the MFQI.

$$\Delta R_{\text{EM}}^+ = [R_{\text{EM}}(\phi^1) - R_{\text{EM}}(\phi^c) \quad R_{\text{EM}}(\phi^2) - R_{\text{EM}}(\phi^c) \quad \cdots \quad R_{\text{EM}}(\phi^n) - R_{\text{EM}}(\phi^c)]^T \quad (25)$$

$$\Delta R_{\text{EM}}^- = [R_{\text{EM}}(\phi^{n+1}) - R_{\text{EM}}(\phi^c) \quad R_{\text{EM}}(\phi^{n+2}) - R_{\text{EM}}(\phi^c) \quad \cdots \quad R_{\text{EM}}(\phi^{2n}) - R_{\text{EM}}(\phi^c)]^T \quad (26)$$

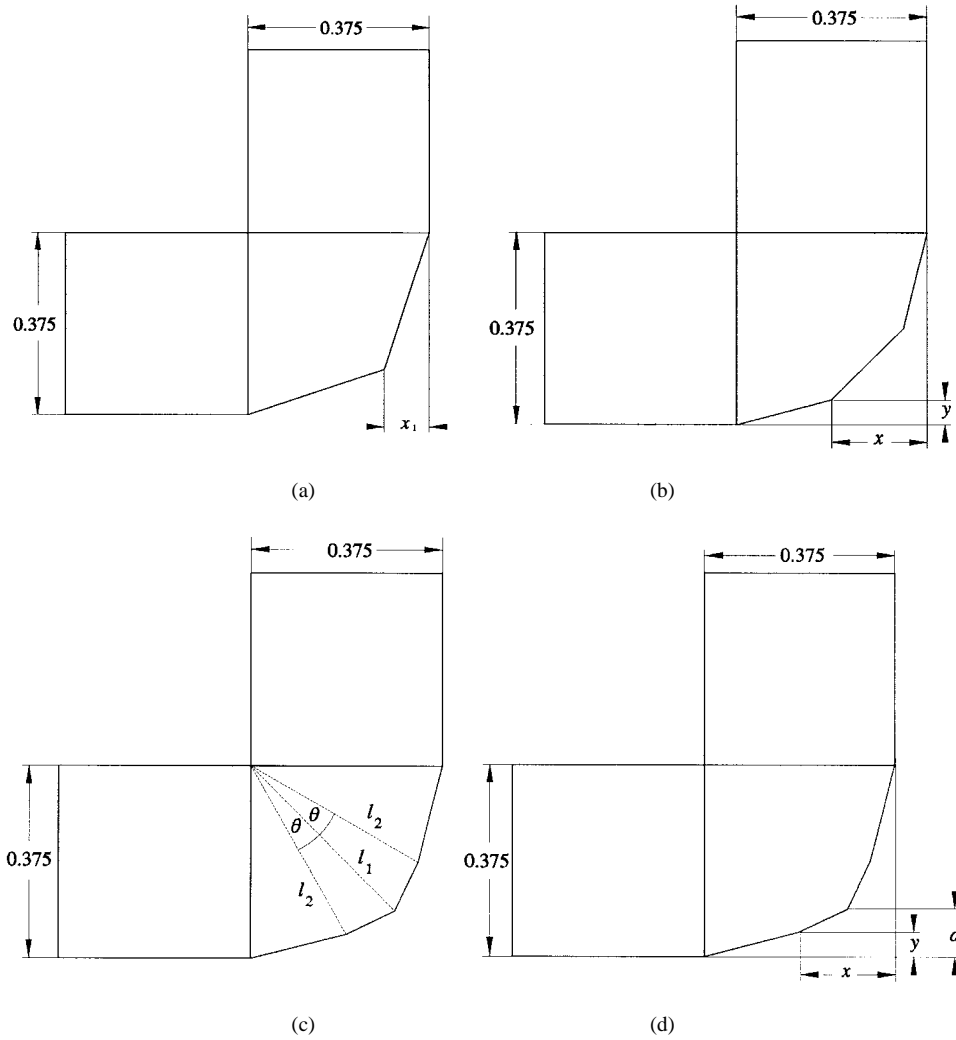


Fig. 6. Additional optimized geometries with optimization variables marked. (a) Two-section miter. (b) Three-section miter. (c) Four-section miter, Case A. (d) Four-section miter, Case B.

When a specific θ_i is zero, one excludes the corresponding base point from the interpolation base. From (19) and (29) it is obvious that the contribution of these base points to the interpolation formula is equal to zero.

VII. AUTOMATIC DESIGN OPTIMIZATION OF MITERED BENDS

As an illustration of fully 3-D EM optimization, results for waveguide bends are presented. The bend is a simple EM structure, used to change the direction of a waveguide run. The geometry of the single-section E -plane mitered bend [45] is sketched in Fig. 2. Symmetrical bends were analyzed, with the standard WR-75 as the input and output waveguides. The bend angle was kept fixed at 90° . In this analysis all edges are sharp, although in a practical design, corners may have a round shape. The design specification is set for return loss over the full bandwidth, namely,

$$\text{return loss} \geq 40 \text{ dB}, \quad \text{for } 9 \text{ GHz} \leq f \leq 15 \text{ GHz}.$$

The FEM appears to be the most suitable EM method for analyzing waveguide bends [45], capable of handling arbitrary geometries, including those with rounded edges.

First, a brute-force design of the structure shown in Fig. 2 was performed. The optimization variable d , the position of the miter, is defined in Fig. 3. Projects for various values of the parameter d were “manually” generated and Maxwell Eminence was run for each project. Fig. 4 shows results for d varied from 0.05 to 0.35 in with a step of 0.05 in. None of the designs satisfied the specifications, and from the diagram one can see that a significant portion of computational effort could be saved. More bluntly, hours of computation time were considered wasted.

A. Single-Section Miter

Automated design optimization is performed using Em-pipe3D on a Sun SPARCstation 10 with 32 Mbytes RAM. A standard gradient-based minimax optimization has been performed. The starting value of the design parameter was taken as $d = 0.1$ in. It was allowed to change between 0–0.375 in, with the discretization step $\delta = 0.025$ in. The solution, $d_{\text{opt}} = 0.2897$ in, was reached after 14 iterations. The total CPU time was about 23 h, when the convergence criterion for Maxwell Eminence (the allowable delta S) was set to 10^{-4} using no more than nine adaptive steps. Relaxing the

TABLE I
MULTISECTION MITERED BENDS SUMMARY OF OPTIMIZATION RESULTS

Sections	Case	Iterations	CPU time	Optimized Values		
1		11	23	$d=0.289$		
2		14	19	$x_1=0.133$		
3		30	15	$x=0.225$	$y=0.065$	
4		12	37	$l_1=0.343$	$l_2=0.33$	
4	A	17	51	$l_1=0.343$	$l_2=0.33$	$\theta=22.49$
4	B	22	98	$d=0.131$	$x=0.281$	$y=0.054$

CPU time is in hours on a Sun SPARCstation 10 with 32 MB RAM.
Values of all optimization variables (d , x_1 , x , y , l_1 and l_2) are in inches, except the angle θ which is in degrees.

convergence criterion, or coarse grid meshing, would speed up the computations at the expense of reduced accuracy.

It is important to note that 14 iterations were performed using only nine Maxwell Eminence simulations, for which the computed S parameters were linearly interpolated using (19). The response of the optimal structure is presented in Fig. 5. It is clear, however, that the design goal could not be achieved.

B. Further Refinement of the Design

The next step in the design process was to refine the geometry and change the number of bend sections. The number of sections were increased up to four, as is depicted in Fig. 6. The optimization variables used are also illustrated in the same figure. Three cases were considered for the four-section miter. First, only the distances l_1 and l_2 were changed from Fig. 6(c), while the angle θ was kept fixed at $\theta = 22.5^\circ$. In the second optimization θ was also used as a design variable, but the design response was not sensitive with respect to change in θ at the specified parameter value. The third set of results was obtained by redefining the optimization variables, as shown in Fig. 6(d). The latter two cases with three optimization variables are referred to as cases A and B.

Fig. 7 shows the optimal geometries for the mitered bends, while Fig. 8 indicates how the corresponding reflection coefficient of optimal one-, two-, and three-section miter meets the specification. It is clear that the two-section miter provides an excellent performance, with return loss well above 40 dB.

The number of sections was then increased to four. The simulation results were almost identical for cases A and B. Fig. 9 presents the responses of the optimal structures. The optimal geometries are practically the same and indistinguishable from the optimized two-section mitered bend. In all cases, the return loss responses are far above 40 dB. The authors believe that the difference in results is due to the numerical approximation method and interpolation.

VIII. SM OPTIMIZATION OF WAVEGUIDE TRANSFORMERS

Other waveguiding structures which were optimized are multistep waveguide transformers. They are classical examples of microwave design optimization [46]. Fig. 10 depicts a typical two-section waveguide transformer. Three designs, of two-, three-, and seven-section transformers, respectively,

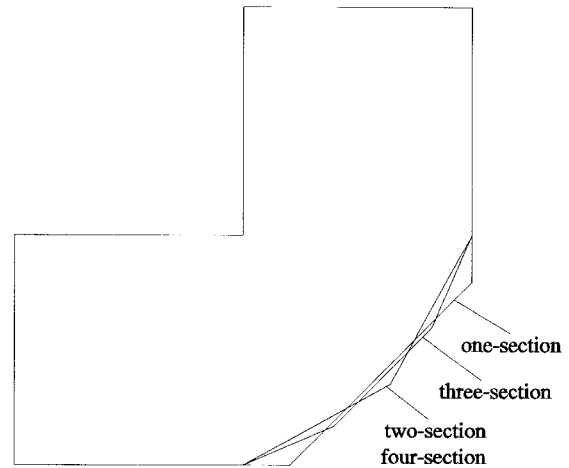


Fig. 7. Geometries of optimal multisection bends. Optimal geometries for all simulation cases of four-section bends are practically identical and are indistinguishable from the optimal two-section bend.

were successfully performed using the automated SM strategy. The variables are the heights and lengths of the waveguide sections.

The SM concept [6] establishes a relation between models in two distinct spaces, namely the optimization space and the EM space. One assumes that the optimization space model is much faster to evaluate but less accurate than the EM model. It can be an empirical model or a coarse-resolution EM model. A procedure of fully automating the aggressive SM strategy [7] using a two-level Datapipe architecture has been presented in [2].

Table I summarizes the simulation results.

First, one applies the SM strategy to two empirical models—an “ideal” model which neglects the junction discontinuity effects and a “nonideal” model which includes the junction discontinuity [46]. Figs. 11–13 show the responses before and after SM optimization. The numbers of iterations required to reach the solutions by SM are seven, six, and five, respectively.

The commercial 3-D structure EM simulator HFSS [11] was then embedded into the automated SM optimization loop. The two-section waveguide transformer shown in Fig. 10 is optimized. In this case, however, HFSS is used as the fine EM model while the coarse model is the same as in the

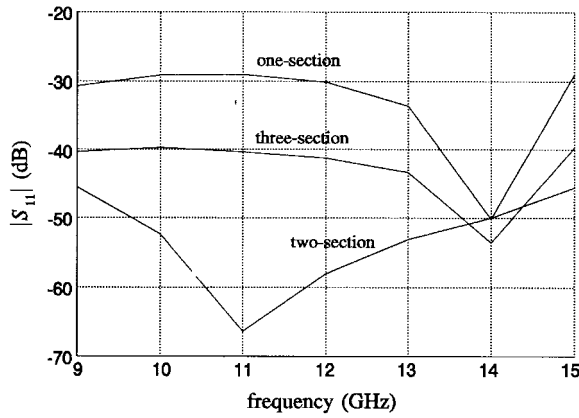


Fig. 8. Comparison of responses of optimal one-, two-, and three-section mitered bends.

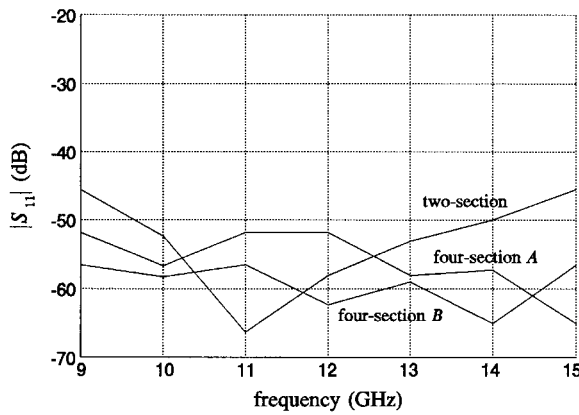


Fig. 9. Responses of optimal two- and four-section bends. The return losses are well above 40 dB (this is already at the simulator’s noise level).

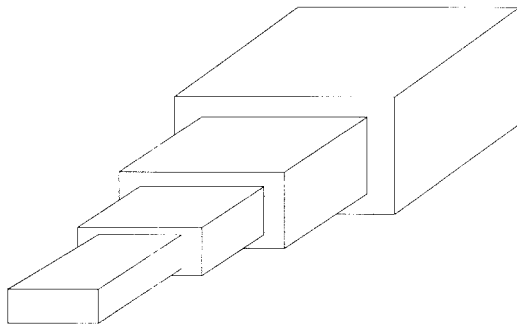


Fig. 10. A typical two-section waveguide transformer.

previous examples, i.e., the “ideal” analytical model. Four variables are involved, namely the heights and lengths of the two waveguide sections. The solution shown in Fig. 14 requires ten SM iterations (hence, ten HFSS simulations).

IX. CONCLUSION

The authors have examined theoretical concepts and formulations relevant to EM optimization of arbitrary structures based on 3-D field simulation. The efficient linear and MFQI interpolation of EM responses have been presented. Using derived interpolation formulas, gradient estimation becomes

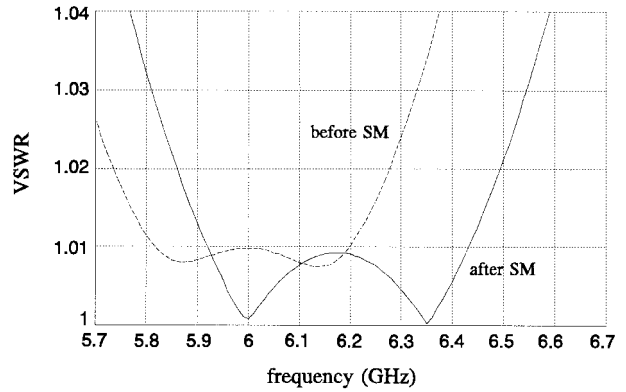


Fig. 11. VSWR response of a two-section waveguide transformer simulated using the nonideal model before and after SM optimization. The response after seven SM iterations is indistinguishable from the optimal ideal response.

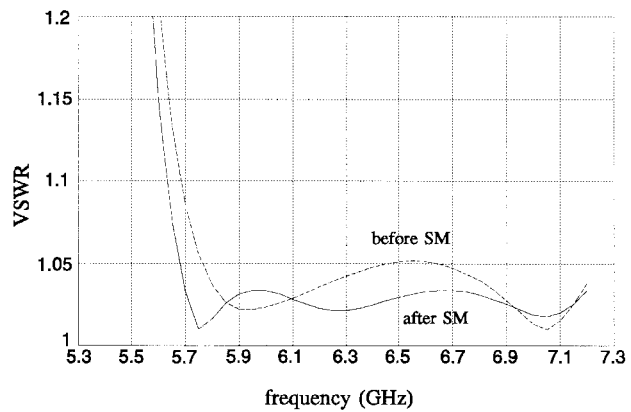


Fig. 12. VSWR response of a three-section waveguide transformer simulated using the nonideal model before and after SM optimization. The response after six SM iterations is indistinguishable from the optimal ideal response.

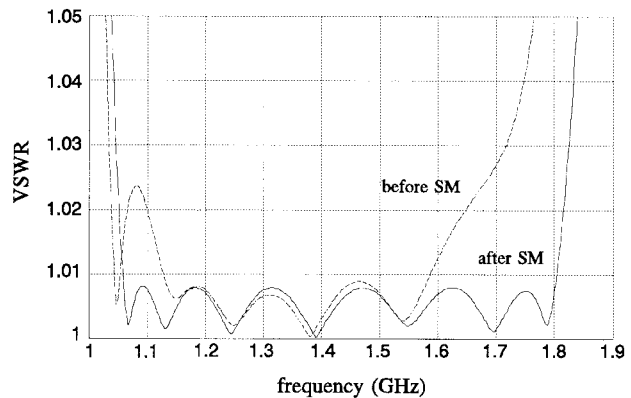


Fig. 13. Voltage standing-wave ratio (VSWR) response of a seven-section waveguide transformer simulated using the nonideal model before and after SM optimization. The response after five SM iterations is indistinguishable from the optimal ideal response.

straightforward. The concept of the intelligent database has been explained. Details of integration of the database system with the authors’ interpolation technique have been presented.

The successful EM optimization of 3-D devices, such as waveguide transformers and mitered bends has been performed

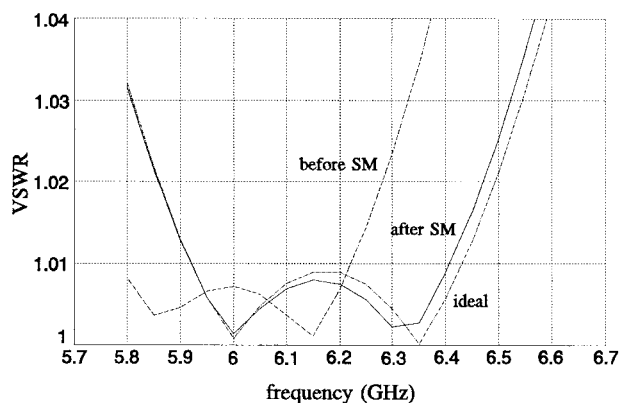


Fig. 14. VSWR response of a two-section waveguide transformer simulated by HFSS before and after ten SM optimization iterations. Also shown is the optimal ideal response.

by driving the commercial 3-D full-wave simulators HFSS and Maxwell Eminence in an optimization loop.

The work in EM optimization of 3-D structures is still considered to be in the early pioneering stages. Much work remains to be done, particularly in the area of design sensitivity evaluation, applied to different numerical approximation methods. Particularly interesting and challenging is the implementation of the adjoint network concept. This approach has the potential of significantly reducing computation time, which is still a principal obstacle in applying optimization techniques in 3-D EM design. Areas still to be explored are the eventual coupling of EM and, for example, thermal problems and the development of more efficient parallelization algorithms.

REFERENCES

- [1] F. Arndt, S. H. Chen, W. J. R. Hoefler, N. Jain, R. H. Jansen, A. M. Pavio, R. A. Pucel, R. Sorrentino, and D. G. Swanson, Jr., "Automated Circuit Design Using Electromagnetic Simulators," in Workshop WMFE, *IEEE MTT-S Int. Microwave Symp.*, (J. W. Bandler and R. Sorrentino, Organizers and Chairmen), Orlando, FL, May 1995.
- [2] J. W. Bandler, R. M. Biernacki, and S. H. Chen, "Fully automated space mapping optimization of 3-D structures," in *IEEE MTT-S Int. Microwave Symp. Dig.*, San Francisco, CA, June 1996, pp. 753–756.
- [3] J. W. Bandler, R. M. Biernacki, S. H. Chen, D. G. Swanson, Jr., and S. Ye, "Microstrip filter design using direct EM field simulation," *IEEE Trans. Microwave Theory Tech.*, vol. 42, pp. 1353–1359, July 1994.
- [4] J. W. Bandler, R. M. Biernacki, S. H. Chen, and P. A. Grobelny, "Optimization technology for nonlinear microwave circuits integrating electromagnetic simulations," *Int. J. Microwave Millimeter-Wave Comput.-Aided Eng.*, vol. 7, pp. 6–28, Jan. 1997.
- [5] J. W. Bandler, R. M. Biernacki, and S. H. Chen, "Parameterization of arbitrary geometrical structures for automated electromagnetic optimization," in *IEEE MTT-S Int. Microwave Symp. Dig.*, San Francisco, CA, June 1996, pp. 1059–1062.
- [6] J. W. Bandler, R. M. Biernacki, S. H. Chen, P. A. Grobelny, and R. H. Hemmers, "Space mapping technique for electromagnetic optimization," *IEEE Trans. Microwave Theory Tech.*, vol. 42, pp. 2536–2544, Dec. 1994.
- [7] J. W. Bandler, R. M. Biernacki, S. H. Chen, R. H. Hemmers, and K. Madsen, "Electromagnetic optimization exploiting aggressive space mapping," *IEEE Trans. Microwave Theory Tech.*, vol. 43, pp. 2874–2882, Dec. 1995.
- [8] J. W. Bandler, R. M. Biernacki, S. H. Chen, and Y. F. Huang, "Design optimization of interdigital filters using aggressive space mapping and decomposition," *IEEE Trans. Microwave Theory Tech.*, this issue.
- [9] M. A. Schamberger and A. K. Sharma, "A generalized electromagnetic optimization procedure for the design of complex interacting structures in hybrid and monolithic microwave integrated circuits," in *IEEE MTT-S Int. Microwave Symp. Dig.*, Orlando, FL, May 1995, pp. 1191–1194.
- [10] *OSA90/hope*, *Empipe*, and *Empipe3D*, Optimization Systems Associates Inc., Dundas, Ont., Canada.
- [11] *HFSS*, HP-EEsof, Santa Rosa, CA.
- [12] *MaxwellEminence*, Ansoft Corporation, Pittsburgh, PA.
- [13] *MagNet*, Infolytica Corporation, Montreal, P.Q., Canada.
- [14] *MSC/EMASMicroWave Lab*, Ansoft Corporation, Pittsburgh, PA.
- [15] M. Koshiba and M. Suzuki, "Application of the boundary-element method to waveguide discontinuities," *IEEE Trans. Microwave Theory Tech.*, vol. MTT-34, pp. 301–307, Feb. 1986.
- [16] C. Nallo, F. Frezza, and A. Galli, "Full wave model analysis of arbitrarily-shaped dielectric waveguides through an efficient boundary-element-method formulation," in *IEEE MTT-S Int. Microwave Symp. Dig.*, Orlando, FL, May 1995, pp. 479–482.
- [17] W. J. R. Hoefler, "Time domain electromagnetic simulation for microwave CAD applications," *IEEE Trans. Microwave Theory Tech.*, vol. 40, pp. 1517–1527, July 1992.
- [18] K. S. Kunz and R. J. Leublers, *The Finite Difference Time Domain Method for Electromagnetics*. Boca Raton, FL: CRC Press, 1993.
- [19] V. J. Brankovic, D. V. Krupcevic, and F. Arndt, "The wave-equation FD-TD method for the efficient eigenvalue analysis and *S*-matrix computation of waveguide structures," *IEEE Trans. Microwave Theory Tech.*, vol. 41, pp. 2109–2115, Dec. 1993.
- [20] T. Itoh, *Numerical Techniques for Microwave and Millimeter Wave Passive Structures*. New York: Wiley, 1989.
- [21] T. Sieverding and F. Arndt, "Field theoretic CAD of open aperture matched T-junction coupled rectangular waveguide structures," *IEEE Trans. Microwave Theory Tech.*, vol. 40, pp. 353–362, Feb. 1992.
- [22] R. F. Harrington, *Field Computation by Moment Methods*. New York: Macmillan, 1968.
- [23] J. C. Rautio and R. F. Harrington, "An electromagnetic time-harmonic analysis of arbitrary microstrip circuits," *IEEE Trans. Microwave Theory Tech.*, vol. MTT-35, pp. 726–730, Aug. 1987.
- [24] D. G. Swanson, Jr., "Simulating EM fields," *IEEE Spectrum*, vol. 28, pp. 34–37, Nov. 1991.
- [25] S. R. H. Hoole, "An integrated system for the synthesis of coated waveguides from specified attenuation," *IEEE Trans. Microwave Theory Tech.*, vol. 40, pp. 1564–1571, July 1992.
- [26] *Touchstone™*, HP-EEsof, Santa Rosa, CA.
- [27] *em*, Sonnet Software, Inc., Liverpool, NY.
- [28] S. Gitosusastro, J. L. Coulomb, and J. C. Sabonnadiere, "Performance derivative calculations and optimization process," *IEEE Trans. Magn.*, vol. 25, pp. 2834–2839, July 1989.
- [29] P. Garcia and J. P. Webb, "Optimization of planar devices by the finite element method," *IEEE Trans. Microwave Theory Tech.*, vol. 38, pp. 48–53, Jan. 1990.
- [30] J. Ureel and D. De Zutter, "Shape sensitivities of capacitances of planar conducting surfaces using the method of moments," *IEEE Trans. Microwave Theory Tech.*, vol. 44, pp. 198–207, Feb. 1996.
- [31] ———, "A new method for obtaining the shape sensitivities of planar microstrip structures by a full-wave analysis," *IEEE Trans. Microwave Theory Tech.*, vol. 44, pp. 249–260, Feb. 1996.
- [32] F. Alessandri, M. Mongiardo, and R. Sorrentino, "New efficient full wave optimization of microwave circuits by the adjoint network method," *IEEE Microwave Guided Wave Lett.*, vol. 3, pp. 414–416, Nov. 1993.
- [33] F. Alessandri, M. Dionigi, and R. Sorrentino, "A fullwave CAD tool for waveguide components using a high speed direct optimizer," *IEEE Trans. Microwave Theory Tech.*, vol. 43, pp. 2046–2052, Dec. 1995.
- [34] D. N. Dyck, D. A. Lowther, and E. M. Freeman, "A method of computing sensitivity of electromagnetic quantities to changes in materials and sources," *IEEE Trans. Magn.*, vol. 30, pp. 341–344, Sept. 1994.
- [35] J. Simkin and C. W. Trowbridge, "Optimizing electromagnetic devices combining direct search methods with simulated annealing," *IEEE Trans. Magn.*, vol. 28, pp. 1545–1548, Mar. 1992.
- [36] S. Russenschuck, "Synthesis, inverse problems and optimization in computational electromagnetics," *Int. J. Numer. Modeling*, vol. 9, pp. 45–57, Jan.–Apr. 1996.
- [37] C. S. Koh, O. A. Mohammed, and S. Y. Hahn, "Nonlinear shape design sensitivity analysis of magnetostatic problems using boundary element method," *IEEE Trans. Magn.*, vol. 31, pp. 1944–1947, May 1995.
- [38] I. Park, B. Lee, and S. Y. Hahn, "Sensitivity analysis based on analytic approach for shape optimization of electromagnetic devices: Interface problem of iron and air," *IEEE Trans. Magn.*, vol. 27, pp. 4142–4145, Sept. 1991.
- [39] J. Kim, H. B. Lee, H. K. Jung, S. Y. Hahn, C. Cheon, and H. S. Kim, "Optimal design technique for waveguide device," *IEEE Trans. Magn.*, vol. 32, pp. 1250–1253, May 1996.

- [40] H. B. Lee, H. K. Jung, S. Y. Hahn, C. Cheon, and H. S. Kim, "An optimum design method for eigenvalue problems," *IEEE Trans. Magn.*, vol. 32, pp. 1246–1249, May 1996.
- [41] D. A. Lowther, "Knowledge-based and numerical optimization techniques for the design of electromagnetic devices," *Int. J. Numer. Modeling*, vol. 9, pp. 35–44, Jan.–Apr. 1996.
- [42] J. W. Bandler, R. M. Biernacki, S. H. Chen, P. A. Grobelny, and S. Ye, "Yield-driven electromagnetic optimization via multilevel multidimensional models," *IEEE Trans. Microwave Theory Tech.*, vol. 41, pp. 2269–2278, Dec. 1993.
- [43] R. M. Biernacki and M. A. Styblinski, "Efficient performance function interpolation scheme and its application to statistical circuit design," *Int. J. Circuit Theory Appl.*, vol. 19, pp. 403–422, July–Aug. 1991.
- [44] R. M. Biernacki, J. W. Bandler, J. Song, and Q. J. Zhang, "Efficient quadratic approximation for statistical design," *IEEE Trans. Circuits Syst. XX*, vol. 36, pp. 1449–1454, Nov. 1989.
- [45] J. Uher, J. Bornemann, and U. Rosenberg, *Waveguide Components for Antenna Feed Systems: Theory and CAD*. Norwood, MA: Artech House, 1993, pp. 163–174.
- [46] J. W. Bandler, "Computer optimization of inhomogeneous waveguide transformers," *IEEE Trans. Microwave Theory Tech.*, vol. MTT-17, pp. 563–571, Aug. 1969.

John W. Bandler (S'66–M'66–SM'74–F'78), for a photograph and biography, see this issue, p. 711.

Radoslaw M. Biernacki (M'86–SM'86–F'96), for a photograph and biography, see this issue, p. 766.

Shao Hua Chen (S'84–M'85–SM'95), for a photograph and biography, see this issue, p. 766.

Louis W. Hendrick received the B.S. and M.S. degrees in electrical engineering from the University of California, Berkeley, and the University of Southern California, Los Angeles, in 1975 and 1984, respectively.

In 1975, he joined the Space and Communications Group of Hughes Aircraft Company, Los Angeles, CA, where he has worked as a Production, Design, and Research Engineer in the passive microwave components area. His research interests include modeling and design of filters, multiplexers, and associated passive devices for satellite communication systems.



Dževat Omeragić (S'90–M'92) received the Dipl.-Ing. and M.Eng. degrees in electrical engineering from the University of Sarajevo, Bosnia-Herzegovina, and the Ph.D. degree from McGill University, Montreal, Canada, in 1986, 1990, and 1994, respectively.

From 1986 to 1990, he was a Research Engineer and Assistant with the Department of Electrical Engineering, University of Sarajevo, working in CAD in electrical power engineering, electromagnetic transients in HV networks, and electric and magnetic field computation. He joined Computational Analysis and Design Laboratory and the Department of Electrical Engineering, McGill University, as a graduate student in 1990. He held a NSERC WUSC Fellowship for the academic year 1990 to 1991. From 1994 to 1996, he was a Post-Doctorate Fellow and Research Associate at McGill University. He joined the Simulation Optimization Systems Research Laboratory and the Department of Electrical and Computer Engineering, McMaster University, in 1996. In 1997 he joined Optimization Systems Associates, Inc., (OSA) as a Research Engineer. His research interests include computational electromagnetics, optimization and applied numerical analysis, FEM's, and CAD of microwave and low-frequency devices.

Dr. Omeragić is a member of the International Compumag Society. He was awarded an NSERC Industrial Research Fellowship with OSA in 1997.